ELSEVIER

International Journal of Mass Spectrometry 218 (2002) 11–18

International Journal of Mass Spectrometry

www.elsevier.com/locate/ijms

Fragmentation of CF_4^{2+} dication from threshold to 120 eV

Toshio Masuoka*, Atsuo Okaji, Ataru Kobayashi

Department of Applied Physics, Graduate School of Engineering, Osaka City University, Sugimoto 3-3-138, Sumiyoshi-ku, Osaka 558-8585, Japan

Received 7 January 2002; accepted 21 March 2002

Abstract

Fragmentation of the doubly charged CF_4^{2+} ion has been studied in the photon-energy region from threshold to 120 eV by using time-of-flight (TOF) mass spectrometry and photoion–photoion coincidence (PIPICO) technique together with synchrotron radiation as a continuum light source. Ion branching ratios for the individual ions (CF_3^{2+}, CF_2^{2+}) and ion pairs ($F^+ + CF_3^+$, $F^+ + CF_2^+$, $F^+ + CF^+$, $C^+ + F^+$), produced from the parent CF_4^{2+} dication, were determined separately from those of the CF_4^+ ion. The ion branching ratios of CF_4^{2+} were differentiated with respect to the incident photon energy. The results obtained by this analytical photoion spectroscopy clearly show fragmentation pathways of the CF_4^{2+} dication, which are observed for the first time in the present study. These pathways are discussed by comparing with calculated electronic states of the CF_4^{2+} dication. (Int J Mass Spectrom 218 (2002) 11–18)

Keywords: Fragmentation; Dication; Carbon tetrafluoride; Ion branching ratios; Synchrotron radiation

1. Introduction

Molecular ions have been widely studied by many experimental methods because of their importance in fundamental physics and chemistry as well as in planetary atmospheres. These methods include X-ray and ultraviolet photoelectron spectroscopy, mass spectrometry, threshold photoelectron–photoion coincidence (TPEPICO) spectroscopy, and threshold electron-fluorescence coincidence technique. These experiments have provided a great deal of our knowledge, such as the dynamics of the production and decay pathways of the ground and excited states of singly charged molecular ions. The references for these methods applied to the CF_4^+ ions have been cited in [1].

As the photon energy is increased, double ionization occurs either by a direct process or via an Auger decay. Actually, the production and dissociation dynamics of doubly charged ions is one of the recent topics in atomic and molecular physics. The CF_4^{2+} dication has received much attention recently by the advent of synchrotron radiation. Recently Hall et al. [2] reported the threshold for double ionization to be 37.5 ± 0.5 eV using threshold photoelectron(s) coincidence (TPEsCO) spectroscopy and presented direct information on the two-hole states of CF_4. Experimental information on the CF_4^{2+} dication has also been obtained via Auger electron spectroscopy (AES) [3] and double-charge-transfer (DCT) spectroscopy [4,5]. The CF_4^{2+} dication dissociates into two ionic fragments (plus neutrals). These fragmentation processes are examined by photoion–photoion coincidence (PIPICO) [6] and photoelectron–photoion–photoion

* Corresponding author.
E-mail: masuoka@a-phys.eng.osaka-cu.ac.jp

1387-3806/02/$ – see front matter
PII S1387-3806(02)00642-5

(PEPIPICO) [7,8] experiments. Among these experiments, Codling et al. [8] determined the thresholds for the ion-pair formation of CF_4^{2+} into $F^+ + CF_3^+$ (37.6 eV), $F^+ + CF_2^+$ (42.4 eV), $F^+ + CF^+$ (47.5 eV) and $C^+ + F^+$ (62.0 eV), and tentatively correlated these thresholds with specific two-hole states of CF_4 calculated by Larkins and Tulea [9]. However, the fragmentation processes of the CF_4^{2+} dication have not been examined in detail.

In this paper, the ion branching ratios of the CF_4^{2+} dication separately determined from those of CF_4^+ are presented in the energy region from threshold to 120 eV. The ion branching ratios were differentiated with respect to the incident photon energy. The results obtained by this analytical photoion spectroscopy clearly show fragmentation pathways of the CF_4^{2+} dication. These pathways are discussed by comparing with the calculated electronic states of the CF_4^{2+} ion [9,10].

2. Experiment

A time-of-flight (TOF) mass spectrometer was used to measure photoionization mass spectra and PIPICO spectra at the Ultraviolet Synchrotron Orbital Radiation (UVSOR) facility of the Institute for Molecular Science (IMS) in Okazaki in the 37–120 eV region with Al (37–70 eV) optical filter (no filter above 72.5 eV). The details of the TOF mass spectrometer and the associated electronic apparatus used in the present experiments have been described elsewhere [11–13]. The TOF mass spectra and PIPICO spectra were measured at an angle of ∼55° with respect to the plane of the storage ring to minimize any effects of anisotropic angular distributions of fragment ions [14] with 1, 2, and 2.5 eV intervals in the energy regions 37–50, 50–70, and 70–120 eV, respectively. To measure the ion branching ratios accurately by mass spectrometry at excitation energies, where single and double photoionization take place concomitantly, the radio frequency (rf) signal (90.115 MHz) of the storage ring operated in a single-bunch mode (the time between adjacent photon bunches is 177.6 ns) was used as the start pulse of a time-to-amplitude converter (TAC) by reducing the frequency appropriately [1]. If the photoelectron signal (not energy selected) was used as a start pulse for the TAC, the different numbers of ejected photoelectrons in single and double photoionization cause an overestimation of the number of ions produced in double photoionization because the probability of forming one output pulse in the electron detector (CEM) is higher for two electrons hitting simultaneously than for one electron [15]. A typical example of the TOF mass spectra is shown in Fig. 1 which is complicated because two or three bunches pass in front of the beam line in the time range shown in the figure, and corresponding sets of the mass spectrum are recorded. The origin of the extra peaks below 45 ns in the figure is not clear at present. In the measurements of PIPICO spectra, the photoion signals detected by a microchannel plate (MCP) were fed into both the start and stop inputs of the TAC. The band pass of a constant-deviation grazing incident monochromator was 0.4 Å (92.5–120 eV) and 0.8 Å (37–90 eV), that is, the worst band path was 0.52 eV at 90 eV.

The fragmentation processes of CF_4^{2+} and CF_4^{+*} observed by the present TOF mass spectra (Eq. 1a) and PIPICO spectra (Eq. 1b) are as follows:

$$CF_4 + h\nu \longrightarrow CF_4^{2+} \longrightarrow CF_2^{2+}, CF_3^{2+} \quad (1-\xi_d), \tag{1a}$$

$$\uparrow$$

$$CF_4^{+*} \longrightarrow C^+ + F^+,\ F^+ + CF^+,\ F^+ + CF_2^+,\ F^+ + CF_3^+ \quad (\xi_d), \tag{1b}$$

where ξ_d is the dissociation ratio of the CF_4^{2+} and CF_4^{+*} ions into two ionic fragments. In these processes, autoionization of super excited states of mono-cations (CF_4^{+*}) may be possible as indicated. It may also be possible that autoionization takes place after dissociation of CF_4^{+*}. This latter process is not explicitly presented in the above equations. Only the final dissociation products in a microsecond time scale are indicated for simplicity. For the ion-pair production (Eq. 1b), the heavier ion of a

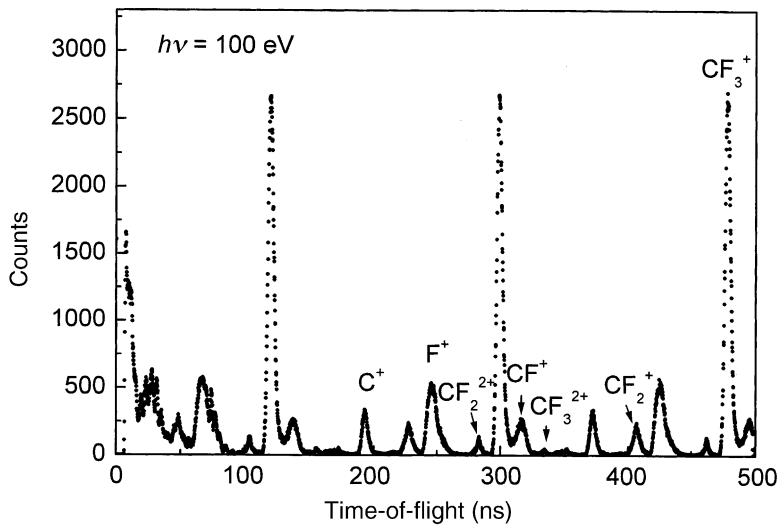

Fig. 1. Time-of-flight mass spectrum measured at a photon energy of 100 eV by using the rf signal of the storage ring as a start input of a TAC. The spectrum is complicated because of the presence of two or three mass peaks, each corresponding to one particular type of ion.

pair may not be counted in a TOF mass spectrum if the ion-detection efficiency is high. This is because the lighter ion stops the TAC. Since we evaluate that the ion-detection efficiency of the MCP used at UVSOR is of the order of a few percent, the heavier ion is detected with almost the same efficiency as the lighter ion. The low ion-detection efficiency of the MCP is partly due to an aging effect caused by using the same detector for a long period and partly due to no use of a mesh in front of the MCP which is usually used to produce a retarding field for photoelectrons ejected to the opposite side of the ion detector. Even though the ion-detection efficiency of the MCP is low, it should be noted that this does not affect the quality of the mass and PIPICO spectra. Instead, it only increases the accumulation time of the spectra to attain necessary counting statistics. At 50 eV, for example, the PIPICO rate was ∼40 counts/s and the data acquisition time was 2000 s. At this energy, the weakest peak is $F^+ + CF^+$ and the integrated PIPICO count of this peak was 1354, whereas the background count due to false coincidences was 1302. Thus, the *S*/*N* ratio was ∼1 and the statistical uncertainties of both the counts were 2.7 and 2.8%, respectively. The total uncertainty was 3.9%. Our criterion for the data acquisition is that the data accumulation is continued until the total counts of a weakest peak (excluding the background) exceed 1000 counts for the mass and PIPICO measurements, except for the spectra measured at energies near the thresholds and very weak peaks particularly in the mass spectra.

3. Data analysis

Details of the determination of the ion branching ratios for the fragmentation of the parent singly and doubly charged ions have been reported previously [16]. The results for CF_4 will be separately reported elsewhere. The procedure for CF_4 is as follows:

(1) The ratios of double to single photoionization (N_d/N_s or equivalently σ^{2+}/σ^{+}, where N_s and N_d represent the rates of single and double photoionization, respectively) are given as a function of photon energy with the ion-collection-detection efficiency f_i of the TOF mass spectrometer, the ion count rate I, the PIPICO rate C_{II} obtained by integrating the area of PIPICO peaks of all ion-pair productions, and the dissociation ratio ξ_d of the CF_4^{2+} and CF_4^{+*} ions into two ionic

fragments, that is,

$$\frac{N_d}{N_s} = \frac{1}{f_i I \xi_d / C_{II} - (1 + \xi_d)}. \quad (2)$$

(2) The sum of the apparent ion branching ratios for the doubly charged CF_3^{2+} and CF_2^{2+} ions obtained directly from the mass spectrum is expressed in terms of the ratio N_d/N_s and the dissociation ratio ξ_d,

$$R_A(CF_2^{2+} + CF_3^{2+}) = \frac{(1 - \xi_d)N_d}{N_s + (1 + \xi_d)N_d}, \quad (3)$$

where $R_A(CF_2^{2+} + CF_3^{2+}) = R_A(CF_2^{2+}) + R_A(CF_3^{2+})$.

(3) By solving the above two equations, N_d/N_s and ξ_d are determined. ξ_d, for example, is given by

$$\xi_d = \frac{x - R_A - xR_A}{(R_A + 1)x}, \quad (4)$$

where $x = N_d/N_s$.

(4) Finally, the inherent ion branching ratios for the ion-pairs and doubly charged ions produced in double photoionization are obtained from ξ_d and the corresponding PIPICO branching ratios R_p or the ratio of the apparent ion branching ratios in the mass spectra for the doubly charged CF_3^{2+} and CF_2^{2+} ions, that is,

$$R(C^+ + F^+) = \xi_d R_p(C^+ + F^+), \quad (5)$$

$$R(F^+ + CF^+) = \xi_d R_p(F^+ + CF^+), \quad (6)$$

$$R(F^+ + CF_2^+) = \xi_d R_p(F^+ + CF_2^+), \quad (7)$$

$$R(F^+ + CF_3^+) = \xi_d R_p(F^+ + CF_3^+), \quad (8)$$

$$R(CF_2^{2+}) = \frac{(1 - \xi_d)R_A(CF_2^{2+})}{R_A(CF_3^{2+} + CF_2^{2+})}, \quad (9)$$

$$R(CF_3^{2+}) = \frac{(1 - \xi_d)R_A(CF_3^{2+})}{R_A(CF_3^{2+} + CF_2^{2+})}. \quad (10)$$

4. Results and discussion

The ion branching ratios of CF_4^{2+} are shown in Fig. 2. As mentioned in Section 2, the six dissociation channels are observed. The measured appearance potentials for the CF_3^{2+} and CF_2^{2+} ions are 40.7 and 41.7 eV, respectively [1]. The thresholds for the ion-pair productions have been reported by Codling et al. [8] as mentioned in Section 1. Their threshold values were used as a guide in the present data analysis. Since their data have been measured with a small wavelength interval as a function of photon energy, their threshold values are probably more reliable than the present ones which were obtained by extrapolation. Therefore, to avoid unnecessary confusion, our threshold values are not presented.

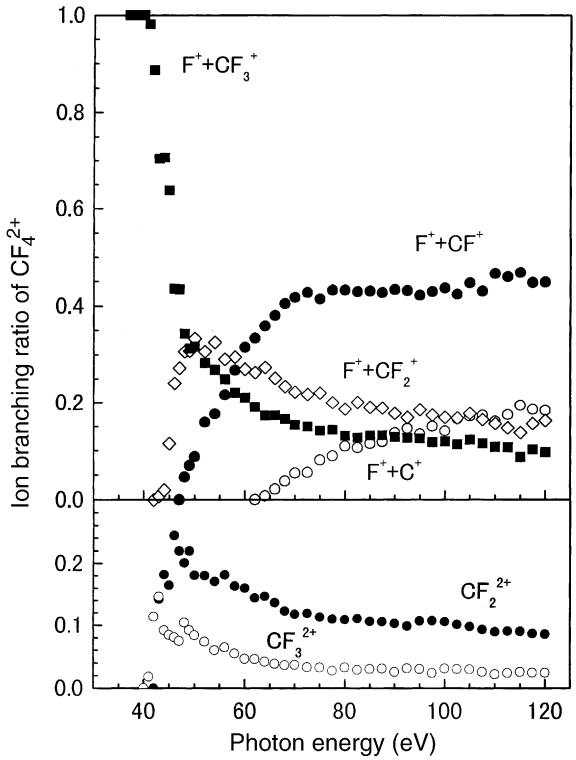

Fig. 2. Ion branching ratios of CF_4^{2+} separately determined from those of CF_4^+.

As can be seen in Fig. 2, the ion branching ratios for the CF_4^{2+} dication show sharp increases at various photon energies. In order to correlate these fragmentation pathways more clearly to the electronic states of CF_4^{2+}, the ion branching ratios were differentiated with respect to the photon energy. This

analytical photoion spectroscopy has been previously described elsewhere [17,18] and further discussed in our recently reported studies of SO_2 and CF_4 [1,19]. That is, the present differential spectra can be considered as a method to visualize better the opening of new dissociation channels, although the energy resolution of the present spectra is rather low.

The resultant photoion spectra are shown in Figs. 3 and 4 with solid curves, in which the positive peaks indicate the fragmentation pathways of CF_4^{2+} to the respective channels. The differential spectra were obtained by the use of ORIGIN (Microcal), in which the derivative was taken by averaging the slopes of the two adjacent pairs of data points. Note that this treatment causes a spectral broadening of the order of the interval between two adjacent data points particularly near the thresholds and leads to a finite value at the

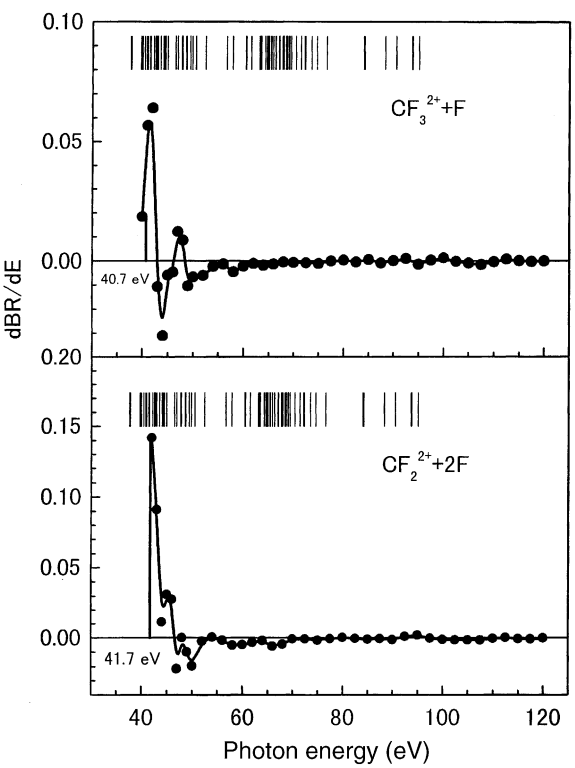

Fig. 3. Differential spectra of ion branching ratios for the CF_3^{2+}+F and CF_2^{2+}+2F fragmentation channels. The thresholds are from [1].

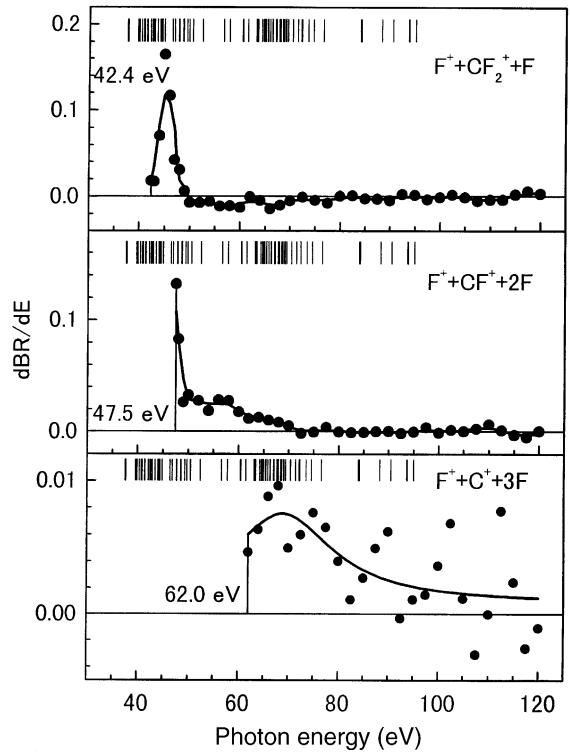

Fig. 4. Differential spectra of ion branching ratios for the $F^+ + CF_2^+ + F$, $F^+ + CF^+ + 2F$, and $C^+ + F^+ + 3F$ fragmentation channels. The thresholds are from [8].

thresholds in the differential spectra. The solid curves in Figs. 3 and 4 are the results of a least-squares fit to an average of three adjacent derivatives with a B-spline function by using ORIGIN. As for the error margins in the differential spectra, one may get an idea from the scattering of the derivatives at high energies where the spectra are essentially flat except for the $C^+ + F^+$ channel. However, it is difficult to generalize the error margins at energies near the thresholds.

The electron configuration of CF_4 in the ground electronic state is [20] $(1a_1{}^2 1t_2{}^6)(2a_1{}^2)(3a_1{}^2 2t_2{}^6)(4a_1{}^2 3t_2{}^6 1e^4 4t_2{}^6 1t_1{}^6)$: $^1A_1$, which corresponds to the F 1s, C 1s, inner- and outer-valence orbitals from the left to the right parenthesis, respectively. The e and t_1 orbitals are exclusively associated with the F atoms [3]. The vertical ionization energies of the five outer-valence orbitals ($1t_1$, $4t_2$, 1e, $3t_2$, $4a_1$) have been

reported to be 16.20, 17.40, 18.50, 22.12, and 25.12 eV, respectively [20], and those correspond to the ion states $\tilde{X}^2T_1$, $\tilde{A}^2T_2$, $\tilde{B}^2E$, $\tilde{C}^2T_2$, and $\tilde{D}^2A_1$. The vertical ionization energies of the two inner-valence orbitals ($2t_2$, $3a_1$) are 40.3 and 43.3 eV [21], corresponding to the ion states $\tilde{E}^2T_2$ and $\tilde{F}^2A_1$.

Larkins and Tulea [9] have calculated the energy of 107 two-hole states associated with the seven outermost orbitals by a semiempirical molecular orbital model. The important bonding orbitals are $4t_2$, $4a_1$, $2t_2$, and $3a_1$ [8]. In the attempt to correlate initial states of the CF_4^{2+} ion with the thresholds for fragmentation mentioned in Section 1, Codling et al. [8] used various simplifying assumptions: the first and the most important one is that no fragmentation occurs when both orbitals are non-bonding or antibonding ($1t_1$, le, $3t_2$), and they shifted the calculated numerals of Larkins and Tulea by 4.8 eV to the lower energy side. The 80 electronic states from the threshold to 95.1 eV shown in Figs. 3 and 4 with vertical bars are those concerned with fragmentation following the above assumption and the energy shift by 4.8 eV. We discuss the present photoion spectra mainly by referring to those 80 electronic states. Hall et. al. [2] have suggested that double ionization mainly occurs via a direct process in the region from the threshold to 50 eV.

4.1. The $CF_3^{2+} + F$ channel (Fig. 3)

This channel is effectively open in the narrow region from the threshold (40.7 eV) to about 43 eV. Although the apparent ion branching ratios of CF_3^{2+} (and CF_2^{2+}) have been differentiated previously [1], no obvious fragmentation pathways were found because of the scattering of the derivatives. On the contrarily, in the present analysis, the clear fragmentation pathways are appreciable. The eight two-hole states, $1e4t_2\ ^3T_1$ (40.8), $1e4t_2\ ^3T_2$ (40.8), $4t_24t_2\ ^3T_1$ (41.0), $4t_24t_2\ ^1E$ (41.4), $4t_24t_2\ ^1T_2$ (41.5), $4t_24t_2\ ^1A_1$ (42.2), $1t_14t_2\ ^1T_1$ (42.5), and $1t_14t_2\ ^1T_2$ (42.7), calculated by Larkins and Tulea [9,10] may be included in this region. That is, the two-electron ejection from the three outermost valence orbitals is related with this channel. The values in the parenthesis indicate the energy of the corresponding states in eV. The second small peak around 47 eV is not probably real. Because the tail of the higher energy side of the peak corresponding to ejection of a single $2t_2$ inner-valence electron continues up to about 46 eV [21], this channel is presumably enhanced by an Auger rearrangement leading to the CF_4^{2+} ion. Recently, the structure of the CF_3^{2+} ion has been studied by ab initio calculations [22].

4.2. The $CF_2^{2+} + 2F$ channel (Fig. 3)

This channel is efficiently open in the region from the threshold (41.7 eV) to about 47 eV. The 11 two-hole states, $4t_24t_2\ ^1A_1$ (42.2), $1t_14t_2\ ^1T_1$ (42.5), $1t_14t_2\ ^1T_2$ (42.7), $3t_24t_2\ ^3A_1$ (43.0), $1e4t_2\ ^1T_2$ (43.5), $1e4t_2\ ^1T_1$ (44.1), $3t_24t_2\ ^3T_2$ (44.3), $3t_24t_2\ ^3T_1$ (44.5), $3t_24t_2\ ^1E$ (44.9), $4a_11t_1\ ^3T_2$ (46.5), and $3t_24t_2\ ^3E$ (46.9), may be involved in this region. The two-electron ejection from the five outer-valence orbitals is concerned with this channel. Again, this channel may be enhanced by an Auger process involving a $3a_1$ inner-valence electron. Very recently, the stability of the ground and excited states of the CF_2^{2+} ion has been investigated by means of the multi-reference average quadratic-coupled cluster (AQCC) method [23].

4.3. The $F^+ + CF_3^+$ channel

This channel may be open in the narrow region from the threshold (37.6) to 40.7 eV (the threshold of the $CF_3^{2+} + F$ channel), where the six two-hole states, $1t_14t_2\ ^3T_1$ (37.6), $1t_14t_2\ ^3T_2$ (37.8), $1t_14t_2\ ^3E$ (39.6), $1t_14t_2\ ^3A_1$ (39.9), $1t_14t_2\ ^1E$ (40.0), and $1t_14t_2\ ^1A_1$ (40.4), may be included. The threshold is associated with the $1t_14t_2\ ^3T_1$ state [8]. The two-electron ejection from the two outermost valence orbitals is related with this channel. Again, this channel may be enhanced by an Auger process involving a $2t_2$ inner-valence electron. From the consideration of the thermochemical threshold (32.2 eV [24]) and the kinetic energy release (5.0 ± 0.2 eV at 45.1 eV), Codling et al. [8] concluded that the CF_3^+ and F^+ fragments are produced in their ground electronic states.

4.4. The $F^+ + CF_2^+ + F$ channel (Fig. 4)

This channel is effectively open in the region from the threshold (42.4 eV) to about 49 eV. The 14 two-hole states, $1t_14t_2\ ^1T_1$ (42.5), $1t_14t_2\ ^1T_2$ (42.7), $3t_24t_2\ ^3A_1$ (43.0), $1e4t_2\ ^1T_2$(43.5), $1e4t_2\ ^1T_1$ (44.1), $3t_24t_2\ ^3T_2$ (44.3), $3t_24t_2\ ^3T_1$ (44.5), $3t_24t_2\ ^1E$ (44.9), $4a_11t_1\ ^3T_2$ (46.5), $3t_24t_2\ ^3E$ (46.9), $3t_24t_2\ ^1T_1$ (47.7), $4a_14t_2\ ^3T_2$ (47.8), $3t_24t_2\ ^1T_2$ (48.6), and $4a_11t_1\ ^1T_2$ (48.7), may be involved in this region. The threshold may be related with the $4t_24t_2\ ^3T_1$ state (the calculated energy is 41.0 eV) [8]. The two-electron ejection from the five outer-valence orbitals is concerned with this channel. Similar to the CF_2^{2+}+2F and F^++CF_3^+ channels, this channel may also be enhanced by an Auger process involving a $3a_1$ inner-valence electron. The CF_2^+ and F^+ ions are also produced in their ground, electronic, and vibrational states [8].

4.5. The $F^+ + CF^+ + 2F$ channel (Fig. 4)

This channel is efficiently open in the rather wide energy region from the threshold (47.5 eV) to about 72.5 eV. The 47 two-hole states may be included in this region. The threshold may involve the $4t_24a_1\ ^3T_2$ state [8]. The two-electron ejection from the five outer-valence orbitals continues up to 57.8 eV [9,10]. The two-electron ejection in which one electron is removed from the $2t_2$ or $3a_1$ inner-valence orbital starts at 60.4 or 65.4 eV, respectively [9,10]. The F^+ ion may be in an excited state [8].

4.6. The $C^+ + F^+ + 3F$ channel (Fig. 4)

This channel is open in the broad energy region from the threshold (62.0 eV) to above 120 eV. The threshold may result from a direct double ionization process involving the $4t_22t_2\ ^3E$ two-hole state [8]. Two-electron ejection from the inner-valence orbitals takes place in this region, i.e., $2t_22t_2\ ^3T_1$ at 84 eV and $3a_1\ 3a_1\ ^1A_1$ at 95.1 eV, the latter is the highest energy calculated by Larkins and Tulea [9,10]. The result indicates that complete atomization of CF_4^{2+} is the major fragmentation process at higher excitation energies.

5. Conclusion

By combining the TOF and PIPICO spectra, the ion branching ratios of the parent CF_4^{2+} dication have been separately determined from those of CF_4^{2+}. The analytical photoion spectroscopy based on the differentiation of the ion branching ratios of the CF_4^{2+} diction with respect to the incident photon energy clearly reveals the various fragmentation pathways of CF_4^{2+} such as CF_3^{2+}+F, CF_2^{2+}+2F, F^++CF_3^+, F^++CF_2^++F, F^++CF^++2F, and C^++F^++3F. That is, this spectroscopy provides a method to visualize better the opening of new dissociation channels. The present photoion spectra have been discussed mainly by referring to the 80 two-hole states calculated by Larkins and Tulea [9,10].

Acknowledgements

Sincere gratitude is extended to the UVSOR personnel for their assistance during the experiments. This work was supported by the UVSOR Joint Research Program of the Institute for Molecular Science.

References

[1] T. Masuoka, A. Kobayashi, J. Chem. Phys. 113 (2000) 1559.
[2] R.I. Hall, L. Avaldi, G. Dawber, A.G. McConkey, M.A. MacDonald, G.C. King, Chem. Phys. 187 (1994) 125.
[3] R.R. Rye, J.E. Houston, J. Chem. Phys. 78 (1983) 4321.
[4] J.W. Griffiths, F.M. Harris, Int. J. Mass Spectrom. Ion Processes 85 (1988) 69.
[5] F.M. Harris, B.C. Cooper, Int. J. Mass Spectrom. Ion Processes 97 (1990) 165.
[6] D.M. Curtis, J.H.D. Eland, Int. J. Mass Spectrom. Ion Processes 63 (1985) 241.
[7] J.H.D. Eland, L.A. Coles, H. Bountra, Int. J. Mass Spectrom. Ion Processes 89 (1989) 265.
[8] K. Codling, L.J. Frasinski, P.A. Hatherly, M. Stankiewicz, F.P. Larkins, J. Phys. B24 (1991) 951.
[9] F.P. Larkins, L.C. Tulea, J. de Physique. C9(12) 48 (1987) 725.
[10] F.P. Larkins, private communication.
[11] T. Masuoka, T. Horigome, I. Koyano, Rev. Sci. Instrum. 60 (1989) 2179.
[12] T. Masuoka, I. Koyano, J. Chem. Phys. 95 (1991) 909.

[13] T. Masuoka, E. Nakamura, A. Hiraya, J. Chem. Phys. 104 (1996) 6200.
[14] T. Masuoka, I. Koyano, N. Saito, Phys. Rev. A. 44 (1991) 4309.
[15] T. Masuoka, E. Nakamura, Phys. Rev. A. 48 (1993) 4379.
[16] T. Masuoka, J. Chem. Phys. 115 (2001) 264.
[17] T. Masuoka, J. Chem. Phys. 81 (1984) 2652.
[18] T. Masuoka, S. Mitani, J. Chem. Phys. 90 (1989) 2651.
[19] T. Masuoka, Y. Chung, E.-M. Lee, J.A.R. Samson, J. Chem. Phys. 109 (1998) 2246.
[20] C.E. Brundle, M.-B. Robin, H. Basch, J. Chem. Phys. 53 (1970) 2196.
[21] K. Siegbahn, C. Nordling, C. Johansson, J. Hedman, P.F. Heden, K. Hamrin, U. Gelius, T. Bergmark, L.O. Werme, R. Manne, Y. Baear, ESCA Applied to Free Molecules, North Holland, Amsterdam, 1969.
[22] J. Hrušák, N. Sändig, W. Koch, Int. J. Mass Spectrom. 185–187 (1999) 701.
[23] J. Hrušák, Chem. Phys. Lett. 338 (2001) 189.
[24] H.M. Rosenstock, K. Mraxi, B. Steiner, J.T. Herron, J. Phys. Chem. Ref. Data 6 (Suppl. 1) (1977).